Localization of Technetium-99m-Glucarate in Zones of Acute Cerebral Injury

Hiroyuki Yaoita, Toshiisa Uehara, Anna Lisa Brownell, Carlos A. Rabito, Marsood Ahmad, Ban An Khaw, Alan J. Fischman, and H. William Strauss

Division of Nuclear Medicine, Department of Radiology, Massachusetts General Hospital and Harvard Medical School, Boston, Massachusetts

The potential structural similarity of technetium-99m-labeled glucaric acid (^{99m}Tc-glucarate) to that of fructose suggests that this agent may enter cells by a sugar transport system. Studies with LLC-PK1 cells demonstrated inhibition of ^{99m}Tc-glucarate uptake by fructose, confirming this potential relationship. Since anaerobic metabolism can use either glucose or fructose, we hypothesized that ^{99m}Tc-glucarate may concentrate in areas of acute ischemic injury. To test this hypothesis, 63 adult rats with middle cerebral artery (MCA) occlusion followed by reperfusion were injected with ^{99m}Tc-glucarate and in vivo and ex vivo images were acquired. Seven animals were also studied with ^{18}FDG and high resolution PET imaging. The radionuclide images were compared to the results of triphenyl tetrazolium chloride (TTC) staining and conventional histopathology. Thirty-five rats had significant accumulation of ^{99m}Tc-glucarate and no TTC staining (indicating infarction) in the involved hemisphere. Of the remaining 28 rats with TTC staining (suggesting viability) of the involved hemisphere, 16 (57%) had ^{99m}Tc-glucarate accumulation. In the seven rats that were studied with both ^{99m}Tc-glucarate and ^{18}FDG, ^{99m}Tc-glucarate accumulated at the center of the occluded MCA territory while ^{18}FDG activity was decreased in this region. These results suggest that ^{99m}Tc-glucarate is a sensitive marker of acute severe cerebral injury, but its mechanism of localization is probably different from that of ^{18}FDG.

J Nucl Med 1991; 32:272-278

The early, objective, identification of the site and extent of damage in patients with acute cerebral ischemia is difficult. The changes seen on computed tomography (CT) scans or conventional radionuclide brain scans occur relatively late in the process (*1,7*), when therapy may be less efficacious. Recently, magnetic resonance imaging (MRI) (*8–10*) and single-photon emission computed tomography (SPECT) with brain blood flow agents (*11–13*) have been used to define areas of injury earlier in the process. These imaging techniques detect different pathophysiologic process in the ischemic brain tissue. CT reflects alterations of tissue density, conventional radionuclide brain scan examines blood-brain barrier integrity, SPECT using current perfusion agents evaluates regional blood flow, and MRI detects alterations of tissue water (*8–14*).

In other tissues, such as the myocardium, areas of ischemia can be specifically identified using metabolic markers. The decreased availability of oxygen causes an increase in glucose utilization via the anaerobic pathway (*15*). Thus, zones of ischemia can be identified as areas of preserved or relatively increased glucose uptake when images are recorded with the positron-emitting glucose analog, fluorine-18-fluorodeoxyglucose (^{18}FDG) (*16,17*). In the brain, however, where glucose is the major substrate, injury is associated with a *decrease* in local glucose utilization (*18–21*). In ischemic tissue, extraction of glucose *increases* even though the amount utilized is decreased due to lower blood flow (*18–21*).

Glucaric acid, a 6-carbon dicarboxylic acid, can be labeled with ^{99m}Tc by stannous chloride reduction (*22*). In rats, intravenous injection of insulin increased myocardial uptake of ^{99m}Tc-glucarate (*23*). Another study performed to determine the length of ischemic injury required for ^{99m}Tc-glucarate localization suggested that this agent accumulates in experimental cerebral infarction within 1 hr of carotid embolization (*24*).

The present studies were performed to characterize the relationship of ^{99m}Tc-glucarate accumulation to ischemic cerebral injury. In a subgroup of animals with ischemic injury, both ^{18}FDG and ^{99m}Tc-glucarate images were recorded.

METHODS

Cell Culture and Flux Measurements

LLC-PK$_1$ cells, a cell line with multiple characteristics of renal proximal tubular cells, were cultured on collagen-coated Nucleopore filter as previously described (*25–27*). Cells, plated at 1/10 the saturation density, divided and reached confluency 5 days after plating. Experiments were performed with mature monolayers 7 days after plating. To define the transport

Received Sept. 5, 1990; revision accepted Oct. 30, 1990.

For reprints contact: H. William Strauss, MD, Division of Nuclear Medicine, Massachusetts General Hospital, Fruit St., Boston, MA 02114.

pathway followed by glucarate in LLC-PK_1 cells, two sets of experiments were performed. First, a group of monolayers was incubated with ^{99m}Tc-glucarate (0.1 m*M*) in the absence or presence of 20 m*M* fructose. Second, another group of monolayers was incubated with ^{14}C-fructose (0.1 m*M*) in presence of 20 m*M* glucarate. The influx of ^{99m}Tc-glucarate or ^{14}C-fructose was measured under conditions approaching initial entry rates, usually after 5 min of incubation in the presence of the labeled substratum. After incubation, the monolayers were washed with ice-cold 0.1 *M* $MgCl_2$ for 90 sec and radioactivity was measured. The results were expressed as cpm/mg DNA.

Animal Model

Cerebral ischemia/infarction was induced by the method of Koizumi et al. (*28*) in 63 male Sprague-Dawley rats (200–250 g). Under ketamine anesthesia (0.125 mg/g), the right carotid artery was exposed and a silicon-coated thread was advanced to the origin of the middle cerebral artery (MCA). To induce cerebral ischemia/infarction, the thread was left in situ for 20–120 min. In this model, injury occurs in the cerebral cortex and lateral caudate nucleus of the right hemisphere perfused by the MCA.

Technetium-99m-Glucarate Imaging

One hour after tail vein injection of 3–6 mCi of ^{99m}Tc-glucarate images were recorded with a standard scintillation camera equipped with a pinhole collimator (3 mm insert). The average distance between the collimator and rat skull was about 3 cm (~5 × magnification). Data were obtained in the parieto-basal (similar to vertex view in human brain imaging) and lateral views for 5 min each on a dedicated nuclear medicine computer system. After in vivo imaging, 56 rats were killed by injection of pentobarbital and decapitated. The brains were removed and ex vivo images were recorded in the parieto-dorsal view (opposite to vertex view in human brain imaging) for 5 min using the same collimator.

FDG Imaging

In seven rats (all reperfused for more than 5 hr), an ^{18}FDG study was performed at the conclusion of in vivo ^{99m}Tc-glucarate imaging. A dose of 250–350 μCi of ^{18}FDG was injected intravenously and 30 min later the rats were positioned prone on the imaging table of an experimental single-slice high-resolution PET tomograph, PCR-1 (*29*). This device employs 360 bismuth germanate (BGO) detectors and 90 photomultiplier tubes in a 45-cm diameter ring. Slice thickness is 5 mm and the final reconstructed resolution is 4.5 mm FWHM at the center of the field of view. Images were acquired at 10 bed positions (10 slices). The initial slice was taken at the level of the posterior eye fissure for 600,000 counts. The scanning time of the subsequent images were determined by that of the initial scan corrected for physical decay. After ^{18}FDG imaging, the rats were killed by i.v. injection of ketamine followed by decapitation. Ex vivo images of ^{99m}Tc-glucarate were recorded by 2 hr after positron imaging to permit decay of residual ^{18}F activity.

Technetium-99m-Glucarate Image Analysis

Technetium-99m-glucarate uptake in the right (ischemic/infarcted) hemisphere was compared with uptake in the contralateral hemisphere and scored qualitatively as follows; 0 = no significant increase in uptake relative to the contralateral hemisphere, 1 = significant uptake, 2 = intense uptake. For quantitative analysis, the count density ratio (count density in the injured hemisphere/count density in contralateral hemisphere) was calculated.

FDG Image Processing

Transverse PET images were reconstructed, and reformatted as coronal images. The slices at the mid-portion of the brain were analyzed by region of interest analysis to calculate a ratio of the right MCA area/left MCA area for comparison to the ^{99m}Tc-glucarate data.

Histopathology

Following ex vivo imaging of ^{99m}Tc-glucarate, the brains were sliced into 3-mm thick coronal sections, placed in a freshly prepared solution of triphenyltetrazolium chloride (TTC) and incubated for 30 min at 37°C. Unstained tissue was considered to have suffered irreversible damage (*30–33*).

The percent infarction ([infarcted area/area of right hemisphere]× 100) was measured by planimetry. A representative slice from each brain was fixed with 10% neutral-buffered formalin for 5 days before embedding in paraffin. Paraffin sections (4 μm) were stained with hematoxylin and eosin and examined by conventional light microscopy to detect morphologic changes of cerebral ischemia/infarction.

Distribution of ^{99m}Tc-Glucarate

After TTC staining, the brains were dissected at the level of the caudatoputamen (Fig. 1) to isolate the following structures supplied by the occluded MCA: caudate and putamen (A_r), primary olfactory lobe (B_r), temporal cortex (C_r), and parietal cortex (D_r). In addition, parietal cortex supplied by anterior cerebral artery (ACA) was isolated (E_r). Similarly, the corresponding contralateral areas (A_1-E_1) were also dissected. The incidence of infarction decreased from territory A to E as previously reported (*34*). The specimens were weighed and counted in a well-type gamma counter to determine the count ratio (injured/normal) for each area of the brain.

Comparison of Localization Between ^{99m}Tc-Glucarate and ^{111}In-DTPA

To evaluate the change in blood-brain barrier permeability in the animal model, brain uptake of ^{99m}Tc-glucarate was

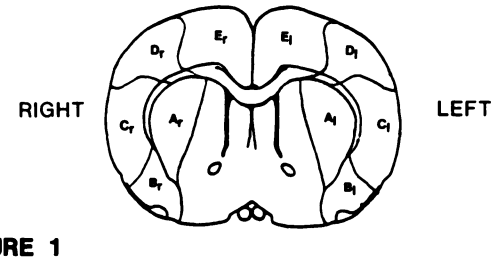

FIGURE 1
Topography of a specimen of rat brain (caudatoputamen level) in which ^{99m}Tc-glucarate content was determined. The right MCA was occluded. A_r = caudate and putamen, B_r = primary olfactory lobe, C_r = temporal cortex, D_r = parietal cortex, E_r = parietal cortex of the ACA territory, and A_1-E_1 = corresponding areas of the contralateral (left) side. Regions B and C represent the core of the occluded MCA territory. Region D is the marginal area and E is the surrounding area.

compared to indium-111-(^{111}In) DTPA uptake. Five rats had occlusion of the right MCA for 30 min. At 3 hr after reperfusion, ^{99m}Tc-glucarate (3 mCi) and ^{111}In-DTPA (0.5 mCi) were injected simultaneously via the tail vein and the animals were killed 1 hr later. The brains were dissected as described above. Radioactivity was measured with a well-type gamma counter and correction for spill-over between the two windows was performed.

Statistical Analysis

All data was expressed as mean ± s.e. Statistical analysis was performed using two-way analysis of variance and Student's t-test.

RESULTS

Cell Culture

Previous studies indicate that the uptake of either ^{99m}Tc-glucarate or ^{14}C-fructose was linear with incubation time up to 15 min. All measurements were made after 5 min of incubation; conditions approaching initial entry. When LLC-PK$_1$ cells were incubated with ^{99m}Tc-glucarate in the presence of 20 m*M* fructose, influx of ^{99m}Tc-glucarate was inhibited by 61% compared to incubation without fructose, from 1149 ± 93 cpm/mg DNA (n = 6) to 450 ± 32 cpm/mg DNA (n = 6). When the cells were incubated with ^{14}C-fructose in the presence of 20 m*M* glucarate, influx ^{14}C-fructose was inhibited by 84% compared to incubation without glucarate, from 5390 ± 338 cpm/mg DNA (n = 6) to 872 ± 56 cpm/mg. DNA (n = 6)

Relationship Between ^{99m}Tc-Glucarate Images and TTC Staining

In 17/20 rats (85%) occluded for more than 1.5 hr and 18/43 rats (42%) occluded for 1 hr or less, the involved hemisphere did not stain with TTC, suggesting infarction (Table 1). Technetium-99m-glucarate localized in the injured hemisphere of all 35 rats that were not stained with TTC (Table 2). In the remaining 28 rats occluded for less than 1.5 hr (Fig. 2), 16 stained with TTC had increased ^{99m}Tc-glucarate localization. Three of these 16 rats (all reperfused for more than 16 hr) showed edema on light microscopy.

The count/density ratio was significantly higher in the group that did not stain with TTC (non-viable) (2.17 ± 0.14) compared to the group that did stain with TTC (1.48 ± 0.09) ($p < 0.0002$).

Distribution of ^{99m}Tc-Glucarate in the Infarction

In 9 rats whose brains were TTC-negative, the ^{99m}Tc-glucarate count density ratio was high in the ipsilateral caudate and putamen (7.20 ± 1.71), primary olfactory lobe (5.10 ± 1.28), and temporal lobe (5.16 ± 1.63); and low in the parietal cortex supplied by the MCA (2.59 ± 0.59) and ACA (1.81 ± 0.44) (Fig. 3). In nine rats whose brains were stained with TTC, the count density ratio showed the same pattern (caudate and putamen: 5.37 ± 2.38; primary olfactory lobe: 2.81 ± 0.69; temporal cortex: 2.25 ± 0.75; parietal cortex (MCA territory): 1.89 ± 0.45; and parietal cortex (ACA territory): 1.34 ± 0.24). Analysis of variance showed a significant main effect of brain area on ^{99m}Tc-glucarate uptake ($p < 0.05$). The uptake ratio at the center of the occluded MCA territory was significantly higher ($p < 0.0002$) than in the other areas.

Changes in Blood-Brain Barrier Permeability After Ischemia

In the group of five rats with 30 min of MCA occlusion, four animals had ischemia (stained with TTC). In this group, %ID/gram of ^{111}In-DTPA was: 0.14 ± 0.11 (caudate and putamen), 0.49 ± 0.30 (primary olfactory lobe), 0.24 ± 0.20 (temporal cortex), 0.11 ± 0.09 (parietal cortex, MCA territory), and 0.08 ± 0.06 (parietal cortex, ACA territory). For ^{99m}Tc-glucarate, the corresponding values were: 0.13 ± 0.08 (caudate and putamen), 0.42 ± 0.35 (primary olfactory lobe), 0.18 ± 0.13 (temporal cortex), 0.13 ± 0.09 (parietal cortex, MCA territory), and 0.07 ± 0.06 (parietal cortex, ACA territory).

Relationship Between ^{99m}Tc-Glucarate and ^{18}FDG Images

The ^{18}FDG count ratios were decreased in three TTC-negative rats, while the ratios were near unity in four TTC-positive animals (Table 3). In general, ^{99m}Tc-glucarate concentrated at the center of the infarcted hemispheres while ^{18}FDG had decreased activity in this area. The count density ratio of ^{99m}Tc-glucarate was 1.64 ± 0.13 in rats with infarction and 1.07 ± 0.06 in rats without infarction while the corresponding values for ^{18}FDG were: 0.83 ± 0.06 (infarcted rats) and 1.01 ± 0.03 (noninfarcted rats).

DISCUSSION

The cell culture data suggest that ^{99m}Tc-glucarate enters cultured renal tubular cells via a fructose transport system. Fructose can contribute to anaerobic metabolism, since it can undergo phosphorylation in similar fashion to glucose (*15*). Also, the observation that ^{99m}Tc-glucarate and 2-deoxyglucose do not compete for the same transport system suggests that the two compounds may have significantly different patterns of in vivo accumulation in some situations. While some insight into the processes involved in ^{99m}Tc-glucarate accumulation in tissue can be gained from experiments with cultured cells, considering the vast difference between renal cells in vitro and rat brain in vivo, it is important that the results of the in vitro experiments should not be over interpreted.

The studies with rats demonstrated minimal accu-

TABLE 1
Relationship Between Occlusion Time, Reperfusion Time, Imaging, and TTC Staining

No.	Occlusion time (hr)	Observation time after RP (hr)	Glucarate image		CDR*	TTC†	FDG image
			In vivo	Ex vivo			
1	0.3	18.5	1+	2+	2.03	1	
2	0.5	0.5	1+	1+	1.82	0	
3	0.5	1		1+	1.81	0	
4	0.5	1	1+	1+	1.78	0	
5	0.5	2	1+	2+	1.75	0	
6	0.5	3.3	–	–	1.33	0	
7	0.5	3.3	2+	2+	2.83	0	
8	0.5	3.5	1+	1+	1.65	0	
9	0.5	4.3	–	–	1.06	0	
10	0.5	5.6	1+	2+	3.72	1	
11	0.5	6	1+	2+	2.70	1	
12	0.5	6.5	2+	2+	2.73	1	
13	0.5	7	1+	2+	2.41	1	
14	0.5	16	1+	1+	1.25	0	
15	0.5	19	1+	2+	2.24	0	
16	0.5	19	–	–	1.04	0	
17	0.75	2	2+	2+	1.75	0	
18	1	0.5	1+	2+	1.90	1	
19	1	1	1+	1+	1.71	0	
20	1	1	1+	1+	1.27	2	+
21	1	1	1+	2+	1.78	2	+
22	1	1.3	–	–	1.04	0	–
23	1	1.5	1+	2+	1.78	2	+
24	1	2.5	1+	1+	1.91	1	
25	1	3		2+	1.50	0	
26	1	3	–	–	1.18	0	
27	1	3.5		1+	1.23	0	
28	1	3.5	1+	1+	2.20	0	
29	1	4		2+	1.51	2	
30	1	4	2+	1+	2.05	0	
31	1	5	–	–	1.05	0	
32	1	5.5	–	–	0.42	0	
33	1	6	–	–	1.14	0	
34	1	6	1+	1+	2.38	1	
35	1	8	–	–	1.22	0	
36	1	8	–	–	0.98	0	–
37	1	13	2+	1+	4.47	1	
38	1	15	2+	2+	2.46	1	
39	1	16	2+	2+	1.74	0	–
40	1	16	2+	2+	1.91	1	
41	1	16	1+	1+	1.99	1	
42	1	20	1+	1+	1.71	1	
43	1	20	1+	1+	1.66	1	
44	1.5	0.5	1+	1+	2.02	1	
45	1.5	1.5	2+	1+	3.68	1	
46	1.5	1.5	1+	1+	1.32	1	
47	1.5	3	2+	2+	2.24	2	
48	1.5	3		2+	1.76	1	
49	1.5	3		1+	1.31	0	
50	1.5	13	1+	1+	1.84	1	
51	1.5	16	1+	1+	1.54	2	
52	2	0.3	2+	2+	4.45	2	
53	2	4		1+	1.47	1	
54	2	4	–	–	1.19	0	–
55	2	5		2+	1.56	1	
56	2	6		2+	1.42	2	
57	2	6		2+	2.52	2	
58	2	8		2+	1.93	2	
59	2	72		2+	1.70	2	
60	2	72		2+	3.61	2	
61	2	72		1+	1.29	1	
62	2	72		–	1.09	0	
63	2	72		1+	1.49	1	

* Count density ratio.
† % Infarcted = Unstained Area/Area of Treated Hemisphere × 100; 0: 0%, 1: 1–25%, 2: >26%.
‡ +: decreased ^{18}FDG activity in territory of occludes MCA. –: increased ^{18}FDG activity in territory of occludes MCA.

TABLE 2
Relationship Between ^{99m}Tc-Glucarate Images and TTC Staining

^{99m}Tc-glucarate images	TTC staining	
	Unstained (irreversibly damaged)	Stained
Accumulation	35 (55.6%)	16 (25.4%)
No accumulation	0 (0%)	12 (19%)

mulation of ^{99m}Tc-glucarate in normal brain, suggesting that is not a preferred substrate under these circumstances. However, at sites of reversible (TTC stained) or irreversible (TTC unstained) injury, increased ^{99m}Tc-glucarate concentration was usually observed. When failure of TTC staining was used as the indicator of irreversible injury (*29,30,31*), ^{99m}Tc-glucarate concentrated in all 35 irreversibly damaged hemispheres. On the other hand, of the 28 brains that were stained with TTC, ^{99m}Tc-glucarate concentrated significantly in 16. While TTC staining may be retained in cells that are destined to die, due to incomplete loss of mitochondrial enzyme activity (*31*), the presence of TTC staining suggests that this tissue is viable. Previous studies in cats have demonstrated that mitochondrial enzyme activity changes in TTC-stained specimens after 2.5 hr of ischemia with subsequent reflow, however, in rats, significant mitochondrial changes were observed after only 60 min of ischemia (*29,30*). Histologic examination of the 16 brains stained with TTC revealed slight edema in 3, but most specimens reperfused for a short time did not show distinct changes at the light microscopic level. Previous studies have shown that under some experimental conditions, cellular function can recover after 30 min of ischemia, making it difficult to precisely categorize these specimens (*35*). A study in rats using the same occlusion method as ours demonstrated retained RNA synthesis after 1 hr of MCA occlusion followed by 12 hr of reperfusion; protein synthesis was inhibited at 2 hr after reperfusion (*36*). In our study, 15 of these 16 rats had occlusion of 1 hr or less. These

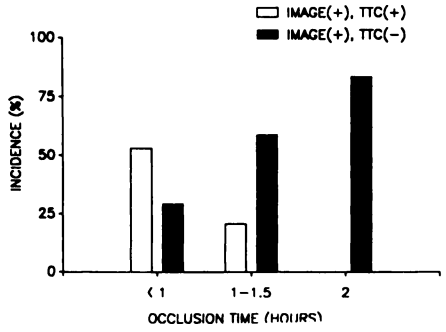

FIGURE 2
Relationship between ^{99m}Tc-glucarate images and TTC staining.

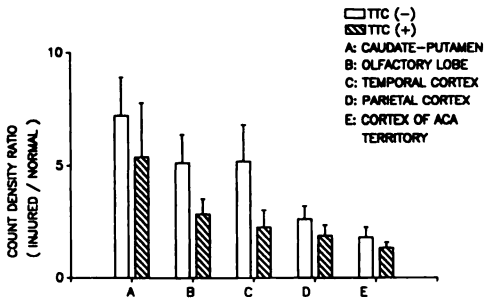

FIGURE 3
Distribution of ^{99m}Tc-glucarate in injured brain.

circumstances suggest that accumulation of ^{99m}Tc-glucarate in the treated hemisphere detects not only irreversible injury but also transient ischemia in tissue which is still viable.

The mechanism of accumulation of ^{99m}Tc-glucarate in ischemic tissue is unknown. It seems unlikely that the generation/unmasking of a specific transport system is involved, and disruption of a permeability barrier seems more plausible.

The present study has demonstrated that blood-brain barrier permeability increases in ischemic viable tissue (30 min MCA occlusion) and that the concentration of ^{99m}Tc-glucarate in mild ischemia is similar to that of ^{111}In-DTPA. Previous studies have reported a marked decrease of regional cerebral blood flow in the territory of the occluded MCA, with flows reached to 11.6–13.0% of the control level during 1 hr of ischemia; following 2 hr of reperfusion, perfusion recovered to 43.3%–46.8% (*30,37*). Since our model is similar to that reported by Abe (*35*), accumulation of ^{99m}Tc-glucarate in ischemic tissue cannot be explained by an increase in regional cerebral blood flow after reperfusion.

Several authors have reported decreased deoxyglucose uptake in infarcted areas of the brain and increased accumulation in surrounding areas (*18–21*). In the present study, the concentration of ^{18}FDG in the involved hemisphere was decreased in three animals and was normal in four. In contrast, significant accumulation of ^{99m}Tc-glucarate was observed in hemispheres with decreased FDG concentration but was equal to

TABLE 3
Relationship Between ^{18}FDG Images and TTC Staining

^{18}FDG images	TTC staining	
	Unstained (irreversibly damaged)	Stained
Decreased activity	3 (42.9%)	0 (0%)
Normal activity	0 (0%)	4 (57.1%)*

* Includes one case in which a small infarction was detected by histopathology.

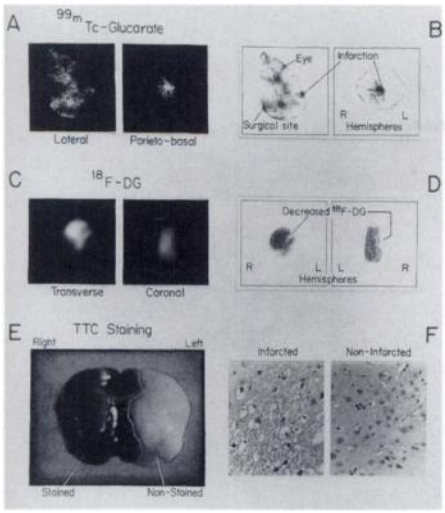

FIGURE 4
Representative case of a rat in which the MCA was occluded for 1 hr before reperfusion. (A) ^{99m}Tc-glucarate images (left: lateral projection, right parieto-basal projection) acquired 2 hr after reperfusion, demonstrating intense focal accumulation of radionuclide in the right hemisphere. (B) Anatomic landmarks corresponding to the images on the left. (C) ^{18}FDG images (left: coronal, right: transverse) acquired 5 hr after reperfusion, demonstrating decreased activity in the right hemisphere. (D) Anatomic landmarks corresponding to the images on the left. (E) TTC staining of a brain section at the caudatoputamen level, demonstrating a large area of infarction in the right hemisphere. (F) Photomicrographs (H & E section, 400×) of infarcted (left) and normal (right) cerebral cortex. In the infarcted cortex, areas of edema and neuronal shrinkage were clearly visible.

the contralateral side in animals with normal histologic findings and normal ^{18}FDG uptake. The discordance between the distribution of ^{99m}Tc-glucarate and ^{18}FDG indicates that the mechanism by which ^{99m}Tc-glucarate acts as a marker of acute cerebral injury is not related to being a glucose analog.

REFERENCES

1. Ramsey RG, Quinn III JL. Comparison of accuracy between initial and delayed Tc-99m-pertecnetate brain scans. *J Nucl Med* 1972;13:131–134.
2. Wolfstein RS, Tanasescu D, Sakimura IT, Waxman AD, Siemsen JK. Brain imaging with Tc-99m-DTPA: a clinical comparison of early and delayed studies. *J Nucl Med* 1974;15:1135–1137.
3. Waxman AD, Tanacesu D, Siemsen JK, Wolfstein RS. Tc-99m-glucoheptonate as a brain-scanning agent: critical comparison with pertechnetate. *J. Nucl Med* 1976;17:345–348.
4. Rollo FD, Cavalieri RR, Born M, Blei L, Chew M. Comparative evaluation of Tc-99m-GH, Tc-99mO4, and Tc-99m-DTPA as brain imaging agents. *Radiology* 1977;123:379–383.
5. Ryerson TW, Spies SM, Singh NB, Zeman RK. A quantitative clinical comparison of three Tc-99m labeled brain imaging radiopharmaceuticals. *Radiology* 1978;127:429–432.
6. Cowan RJ. Conventional radionuclide brain imaging in the era of transmission and emission tomography. *Semin Nucl Med* 1986;16:63–73.
7. Calandre L, Gomara S, Bermejo F, Millan JM, Pozo GD. Clinical-CT correlations in TIA, RIND, and strokes with minimum residuum. *Stroke* 1984;15:663–666.
8. Naruse S, Horikawa Y, Tanaka C, Hirakawa K, Nishikawa H, Yoshizaki K. Proton nuclear magnetic resonance studies on brain edema. *J Neurosurg* 1982;56:747–752.
9. Spetzler RF, Zabramski JM, Kaufman B, Yeung HN. Acute NMR changes during MCA occlusion: a preliminary study in primates. *Stroke* 1983;14:185–191.
10. Buonanno FS, Pykett IL, Brady TJ, et al. Proton NMR imaging in experimental ischemic infarction. *Stroke* 1983; 14:178–184.
11. Hellman RS, Collier BD, Tikofsky RS, et al. Comparison of single-photon emission computed tomography with I-123 iodoamphetamine and xenon-enhanced computed tomography for assessing regional cerebral blood flow. *J Cereb Blood Flow Metab* 1986;6:747–755.
12. Holman BL, Jolesz FA, Polak JF, Kronauge JF, Adams DF. Comparison of I-123-IMP cerebral uptake and MR spectroscopy following experimental carotid occlusion. *Invest Radiol* 1985;20:370–373.
13. Brott TG, Gelfand MJ, Williams CC, Spilker JA, Hertzberg VS. Frequency and patterns of abnormality detected by iodine-123 amine emission CT after cerebral infarction. *Radiology* 1986;158:729–734.
14. Seiderer M, Krappel W, Moser E, et al. Detection and quantification of chronic cerebrovascular disease. Comparison of MR imaging, SPECT, and CT. *Radiology* 1989;170:545–548.
15. Lehninger AL. Glycolysis: a central pathway of glucose catabolism. In: *Principles of biochemistry.* New York: Worth Publishers: 1982;397–434.
16. Marshall RC, Tillisch JH, Phelps ME. Identification and differentiation of resting myocardial ischemia and infarction in man with positron computed tomography, ^{18}F-labeled fluorodeoxyglucose and N-13-ammonia. *Circulation* 1983; 67:766–768.
17. Tillisch J, Brunken R, Marshall R, et al. Reversibility of cardiac wall-motion abnormalities predicted by positron tomography. *N Engl J Med* 1986;314:884–888.
18. Nedergaard M, Gjedde A, Diemer NH. Focal ischemia of rat brain: autoradiographic determination of cerebral glucose utilization, glucose content, and blood flow. *J Cereb Blood Flow Metab* 1986;6:414–424.
19. Ginsberg MD, Reivich M, Giandomenico M, Greenberg JH. local glucose utilization in acute focal cerebral ischemia: local dysmetabolism and diascisis. *Neurology* 1977;27:1042–1048.
20. Ginsberg MD, Reivich M. Use of the 2-deoxyglucose method of local cerebral glucose utilization in the abnormal brain: evaluation of the lumped constant during ischemia. *Acta Neurol Scand* 1979;60(suppl 72):226–227.
21. Choki J, Greenberg JH, Jones SC, Reivich M. Correlation between blood flow and glucose metabolism in focal cerebral ischemia in the cat. *J Cereb Blood Flow Metab* 1983;3(suppl 1):399–400.
22. Pak KY, Nedelman MA, Daddona PE. Visualization of experimental tumor model: application of a new Tc-99m-labeled compound [Abstract]. *J Nucl Med* 1989;30:P906.
23. TenKate CI, Fischman AJ, Wilkinson RA, et al. Tc-99m-glucaric acid: a glucose analog. *Eur J Nucl Med* 1990;31:451.
24. Khaw BA, Pak KY, Ahmad M, Nossiff ND, Strauss HW. Visualization of experimental cerebral infarct: application of a new Tc-99m-labeled compound. *Circulation* 1985;78: (suppl) II-140.
25. Rabito CA, Tchao R, Valentich J, Leighton J. Distribution and characteristics of the occluding junctions in a monolayer of a cell line (MDCK) derived from canine kidney. *J Membrane Biol* 1978;43:351–365.
26. Rabito CA, Ausiello DA. Na^+ dependent sugar transport in a cultured epithelial cell line from pig kidney. *J Membrane Biol* 1980;54:31–38.

27. Rabito CA: Localization of the Na^+ sugar cotransport system in a kidney epithelial cell line (LCC PK1). *Biochemica Biophysica Acta* 1981;649:286–296.
28. Koizumi J, Yoshida Y, Nakazawa T, Ooneda G. Experimental studies of ischemic brain edema. A new experimental model of cerebral embolism in rats in which recirculation can be introduced in the ischemia area. *Jpn J Stroke* 1986;8:1–7.
29. Brownell GL, Burnham CA, Chesler DA. High resolution tomograph using analog coding. In: Greiz T, et al, eds. *The metabolism of human brain studied with positron emission tomography.* New York: Raven Press; 1985:13–19.
30. Arsenio-Nunes ML, Hossmann KA, Farkas-Bargeton. Ultrastructural and histochemical investigation of the brain cortex of cat during and after complete ischemia. *Ann Neuropathol* 1973;2:329–344.
31. Brown AW, Brierley JB. Anoxic-ischemic cell change in rat brain: light microscopic and fine-structural observations. *J Neurol Sci* 1972;16:59–84.
32. Liszczak TM, Hedley-Whyte ET, Adams JF, et al. Limitation of tetrazolium salts in delineating infarcted brain. *Acta Neuropathol* 1984;65:150–157.
33. Zervas NT, Geyer RP, Han DH, et al. Can perfluochemicals reduce cerebral ischemia? In: Reivich JF, Hutig HI, eds. *Cerebrovascular diseases.* New York: Raven Press; 1983:409–419.
34. Duverger D, Mackenzie ET. The quantification of cerebral infarction following focal ischemia in the rat: influence of strain, arterial pressure, blood glucose concentration, and age. *J Cereb Blood Flow Metab* 1988;8:449–461.
35. Rehncrona S, Mela L, Siesjo BK. Recovery of brain mitochondrial function in the rat after complete and incomplete cerebral ischemia. *Stroke* 1979:10;437–446.
36. Abe K, Araki T, Kogure K. Recovery from edema and protein synthesis differs between the cortex and caudate following transient focal cerebral ischemia in rats. *J Neurochem* 1988;51(5):1470–1475.
37. Sakurada O, Kennedy C, Jehle JW, Brown JD, Carbin L, Sokoloff L. Measurement of local cerebral blood flow with iodo-C-14-antipyrine. *Am J Physiol* 1978;234:H59–H66.